Biochemical and Biophysical Research Communications 398 (2010) 571–575

Contents lists available at ScienceDirect

Biochemical and Biophysical Research Communications

journal homepage: www.elsevier.com/locate/ybbrc

Design, synthesis, and biological evaluation of 4-(5-dimethylamino-naphthalene-1-sulfon-amido)-3-(4-iodophenyl)butanoic acid as a novel molecular probe for apoptosis imaging

Wenbin Zeng [a,b,*], Weimin Miao [b], Michael Le Puil [c], Guangqing Shi [d], John Biggerstaff [c], George W. Kabalka [b], David Townsend [b]

[a] School of Pharmaceutical Sciences, Central South University, 172 Tongzipo Road, Changsha 410078, China
[b] Graduate School of Medicine, University of Tennessee, 1924 Alcoa Hwy, Knoxville, TN 37920, USA
[c] Center of Environmental Biotechnology, University of Tennessee, 676 Dabney Hall, Knoxville, TN 37996, USA
[d] The Third Xiangya Hospital, Central South University, 168 Tongzipo Road, Changsha 410078, China

ARTICLE INFO

Article history:
Received 22 June 2010
Available online 1 July 2010

Keywords:
Molecular probe
Molecular imaging
Apoptosis
Annexin V

ABSTRACT

Apoptosis (programmed cell death) plays a crucial role in the pathogenesis of many disorders, thus the detection of apoptotic cells can provide the physician with important information to further therapeutic strategies and would substantially advance patient care. A small molecule, 4-(5-dimethylamino-naphthalene-1-sulfonamido)-3-(4-iodo-phenyl)butanoic acid (DNSBA), was designed as a novel probe for imaging apoptosis and synthesized with good yield. The biological characterization demonstrated that DNSBA can be used to specifically and selectively detect apoptotic cancer cells at all stages. DNSBA is also designed as a potential SPECT and PET probe when labeled with radioiodine (I-123, -124, and -131).

1. Introduction

Apoptosis (programmed cell death) plays a crucial role in the pathogenesis of many disorders, such as transplant rejection, cerebral and myocardial ischemia, neurodegenerative diseases, infections, tumor response to chemotherapy and/or radiotherapy. Therefore, the detection of apoptotic cells can provide the physician with important information to further therapeutic strategies and would substantially advance patient care [1–4]. While methods for *in vitro* apoptosis detection are relatively well developed, *in vivo* imaging of apoptosis has only achieved limited success. There are growing interests in the development of novel probes or biomarkers for molecular imaging of apoptosis. To date, Annexin V, a 36 kDa protein, is the most extensively studied probe for *in vivo* apoptosis imaging [5]. Generally speaking, Annexin V is used as the golden standard probe for early apoptosis due to its ability to bind to anionic phospholipid surfaces, in relation with the apoptosis-related externalization of phosphatidylserine (PS) exposed on the membrane surface. A range of Annexin V derivatives (such as dyes and radiochemical labeling conjugations) are used extensively in cell-biology research [6]. However, Annexin V has some drawbacks that diminish its utility in certain and wide applications. For instance, the interaction with this protein requires the presence of a certain concentration of Ca^{2+} ions which is up to 2.5 mM. Meanwhile, Annexin V can associate with membrane surfaces containing negatively charged byproducts of lipid peroxidation, and its lipid binding specificity can be affected by detergents in the medium [7]. Additionally, Annexin even binds to normal cells, and might not have the necessary chemical stability for employment in high-through screening of cancer drugs [8]. Furthermore, other profiles of Annexin V, such as the non-specific biodistribution and slow blood clearance, make it difficult to apply in the clinic [9]. Therefore, a number of small molecules, nanoparticles and peptides have been examined as alternatives to Annexin V [10–14]. Among the small molecules investigated, *N*,*N*′-didansyl-L-cystine (DCC, **1**) and 5-(dimethylamino)-1-naphthalene-sulfonyl-ethylfluoroalanine (NST-732, **2**) have demonstrated great promise (Scheme 1) [15,16].

Recently, we reported the preparation and evaluation of a dansylhydrazone derivative (DFNSH, **3**) as a substitution of Annexin V [17–19]. The straightforward, highly efficient synthesis of the fluorine-18 analog of **3** makes it potentially valuable for positron emission tomography (PET) imaging studies. Iodine-123, iodine-124, and iodine-131 have relative long half-lives when compared to fluorine-18, and are quite useful for non-invasive tomographic imaging studies, including both single photon emission computed tomography (SPECT) and PET. Since our previous work and other literature discovered the dansyl derivatives accumulated inside

* Corresponding author at: School of Pharmaceutical Sciences, Central South University, 172 Tongzipo Road, Changsha 410078, China. Fax: +86 731 8260459.
E-mail address: wbzeng@hotmail.com (W. Zeng).

0006-291X/$ - see front matter © 2010 Elsevier Inc. All rights reserved.
doi:10.1016/j.bbrc.2010.06.120

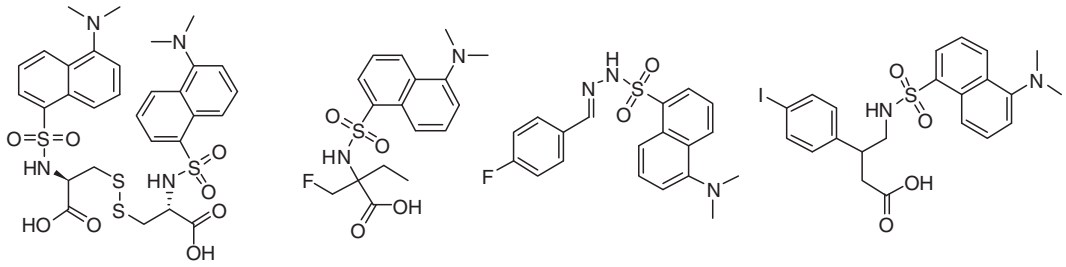

Scheme 1. Dansyl derivatives for imaging apoptosis.

the cytoplasm of the apoptotic cells, we utilize this fluorophore moiety to develop a novel fluorescent probe capable to detect apoptosis. In order to develop a small-molecule probe amenable for radioactive iodine labeling and SPECT/PET scanning for imaging apoptosis, the amino acid derivative, DNSBA (**4**), was designed on a hypothesis with better *in vivo* features, and synthesized in good yield.

2. Materials and methods

2.1. Apparatus and reagents

The chemicals were purchased from Sigma-Aldrich, Acros, or Fisher. All other reagents used in synthesis were commercial products and were used without further purification unless otherwise indicated. Thin-layer chromatography (TLC) was carried out using pre-coated aluminum-backed silica gel, 60 F_{254} TLC plates (E. Merck Company, Darmstadt, Germany) to verify product purities. ^{1}H and ^{13}C nuclear magnetic resonance (NMR) spectra were recorded on a 400 MHz spectrometer (Varian INOVA 400) or a 250 MHz (Bruker AC250) spectrometer. Elemental analyzes were performed at Atlantic Microlab, Inc., Norcross, Georgia.

2.2. In vitro efficacy studies

A series of experiments were performed to evaluate the efficacy of compound **4** in detecting apoptosis in breast cancer MCF-7 cells by comparing **4** to Alexa®488, a fluorescent labeled derivative of Annexin V. Images were obtained using spectral imaging microscopy (ASI, Migdal Ha'Emek, Israel). Actively growing (~80% confluent) MCF7 cells were not stained by DNBSA and Alexa®488 labeled Annexin V. The apoptosis of MCF-7 cells was induced by exposing the cells to 50 nM paclitaxel at 37 °C for 16 h. The apoptotic MCF-7 cells were dually stained with Alexa®488 labeled Annexin V and compound **4** (50 μM in HEPES buffer, 2.5 mM $CaCl_2$, pH 7.4) using a standard protocol [15].

The apoptotic MCF-7 cells stained with Alexa®488-labeled Annexin V and compound **4** were observed using an Applied Spectral Imaging (ASI, Migdal Ha'Emek, Israel) platform-comprised of an Olympus BX61 deconvolution microscope, an ASI interferometer-based spectral head, and a high definition cooled charge-coupled device camera (VDS Vosskuehler GmbH, Osnabrueck, Germany). Images were acquired at 100× and 600× total magnification. A sequential scan of a field of view for a given stained slide was performed using the filter cubes that allow acquisition and separation of the proposed fluorophores (i.e. Alexa®488 and **4**) in two different channels. The excitation and emission characteristics of these fluorophores, and the corresponding filter cubes are used to detect them. In addition, a third image in the same field of view was acquired by differential interference contrast (DIC) to reveal cell structure and morphology. Upon acquisition, each set of three images (one for each fluorophore and DIC) was processed with the AutoDeblur® (Media Cybernetics Inc., Silver Spring, MD) image analysis software for deconvolution (i.e. deblurring) and sharpening. Each image was then presented individually, and an overlay of the fluorescent images with DIC was created to demonstrate the location of both fluorophores into the cells. To conclusively demonstrate the localization of Annexin V on the cell membrane, and of **4** within the cell, three-dimensional (3-D) image stacks of 5 μm depth (encompassing the whole cell's depth) were acquired at 600× total magnification. Each stack was comprised of two series of 25 optical slices (two-dimensional images) obtained as detailed above. One series was acquired for Alexa®488-labeled Annexin V and another for **4**, in the same field of view. A step of 0.2 μm between each optical slice was set in accordance with the Rayleigh depth of field for optimal 3-D resolution. Both stacks for each fluorescent signal were processed with AutoDeblur®. An overlay of both stacks was created and optical slices comprising both fluorophores were presented at 1.2 μm vertical intervals to span the whole depth of the apoptotic cell of interest.

3. Results

The synthesis of the γ-amino acid **4** is outlined in Scheme 2. The iodochalcone **7** was prepared by treatment of acetophenone with 4-iodobenzaldehyde at base condition in 88% yield. Compound **7** was added with 10 equivalents of nitromethane in toluene to produce the crystalline Michael adduct in 90% yield. Baeyer–Villiger oxidation of compound **8** afforded the γ-nitro ester **9** as a colorless solid in 89% yield. γ-Lactam **10** was prepared by treatment of **9** with sodium borohydride in the presence of nickel boride (freshly prepared *in situ* from 1 equivalent of $NiCl_2$ and 5 equivalents of $NaBH_4$ [20]) in methanol at room temperate for 30 min. Hydrolysis of lactam **10** in 5 N aqueous HCl at reflux for 5 h afforded the γ-amino acid hydrochloride salt **11** in 88% yield. Addition of dansyl chloride to this salt under basic conditions gave the desired product **4** in 91% yield. The boron ester **13** could be prepared by the reaction of DNSBA with bis(pinacolato)diboron in the presence of $PdCl_2$(dppf) and KOAc, and be applied to produce radioiodinated **4** using either iodine-123, iodine-124, or iodine-131 under no-carrier-added conditions [21].

3.1. Synthesis of (E)-3-(4-iodophenyl)-1-phenylprop-2-en-1-one (7)

A mixture of acetophenone (481 mg, 4 mmol) and 4-iodobenzaldehyde (967 mg, 4 mmol) in ethanol (15 mL) was added with a solution of NaOH (6 N, 12 mmol) at room temperature. After 1 h, this mixture was cooled by ice, followed by filtration. The residue was washed with cold methanol and recrystallized from methanol to yield a white solid (1.17 g, 88%). ^{1}H NMR ($CDCl_3$). δ (ppm) = 8.03 (m, 2H), 7.78 (m, 2H), 7.70 (m, 6H), 7.35 (d, 1H, J = 8.2 Hz). ^{13}C NMR ($CDCl_3$). δ (ppm) = 189.6, 143.6, 138.1, 134.3, 133.0, 131.4, 128.7,

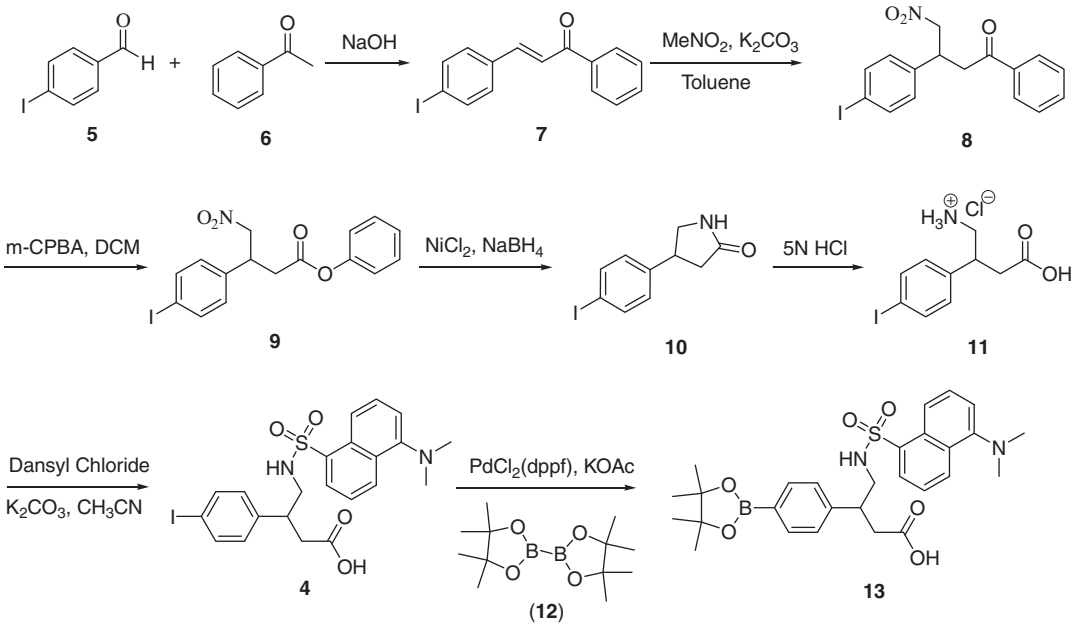

Scheme 2. The synthesis of DNSBA (**4**).

128.5, 127.6, 122.6, 121.5. HR-MS Calcd for $C_{15}H_{11}IO$: 333.9855. Found: 333.9858.

3.2. Preparation of 3-(4-iodophenyl)-4-nitro-1-phenylbutan-1-one (*8*)

A toluene solution (10 mL) of benzyltriethylammonium chloride (20 mg, 0.1 mmol), K_2CO_3 (376 mg, 2 mmol), and **7** (334 mg, 1 mmol) was added with freshly distilled nitromethane (0.54 mL, 10 mmol) at −20 °C. The reaction mixture was stirred at room temperature for 4 h and quenched with icy water. The mixture was extracted with ethyl acetate (20 mL, three times). The combined organic layer was washed with brine, dried over $MgSO_4$, and concentrated under vacuum. The crude products were purified by silica gel flash column chromatography to give **8** (355 mg, 90%). ^{1}H NMR ($CDCl_3$). δ (ppm) = 7.92 (m, 1H), 7.67 (m, 3H), 7.56 (m, 3H), 7.03 (m, 2H), 4.77 (m, 1H), 4.66 (m, 1H), 4.21 (m, 2H), 3.43 (m, 1H). ^{13}C NMR ($CDCl_3$). δ (ppm) = 200.3, 138.1, 133.7, 131.4, 129.8, 129.4, 128.8, 128.7, 128.0, 127.9, 127.1, 93.4, 79.2, 41.2, 38.8. HR-MS Calcd for $C_{16}H_{14}INO_3$: 395.0018. Found: 395.0076.

3.3. Preparation of phenyl 3-(4-iodophenyl)-4-nitrobutanoate (*9*)

To a mixture of 173 mg of *m*-CPBA and 336 mg of $NaHCO_3$ in dichloromethane (10 mL) was added **8** (197, 0.5 mmol). The mixture was stirred at room temperature for 48 h, and then washed with two 10 mL portions of 10% Na_2SO_3 and 20 mL of saturated $NaHCO_3$, followed by the extraction with CH_2Cl_2. The organic layer was dried over Na_2SO_4 and concentrated in vacuum. The residue was purified by silica gel column chromatography to give a white solid **9** (182 mg, 89%). ^{1}H NMR ($CDCl_3$). δ (ppm) = 7.91 (m, 1H), 7.66 (m, 3H), 7.53 (m, 3H), 7.00 (m, 2H), 4.80 (m, 1H), 4.69 (m, 1H), 4.20 (m, 2H), 3.41 (m, 1H). ^{13}C NMR ($CDCl_3$). δ (ppm) = 172.3, 138.0, 133.5, 131.0, 129.5, 128.9, 128.6, 128.1, 127.8, 127.0, 126.1, 91.4, 79.0, 39.2, 36.8. HR-MS Calcd for $C_{16}H_{14}INO_4$: 410.9968. Found: 410.9974.

3.4. Synthesis of 4-(4-iodophenyl)pyrrolidin-2-one (*10*)

Nickel (II) chloride hexahydrate (237 mg, 1 mmol) was added to a stirred solution of **9** (181 mg, 0.5 mmol in 8 mL of methanol) at room temperature. After 5 min, sodium borohydride (190 mg, 5 mmol) was added in five portions. The reaction mixture was stirred at room temperature for 30 min, then filtered in vacuum through Celite, and washed with methanol. The combined solvents were evaporated under reduced pressure. The residue was purified by silica gel column chromatography to yield **10** as a white solid (127 mg, 89%). ^{1}H NMR ($CDCl_3$). δ (ppm) = 7.48 (d, 2H, *J* = 8.5 Hz), 7.15 (d, 2H, *J* = 8.5 Hz), 3.79 (m, 1H), 3.65 (m, 1H), 3.41 (m, 1H), 2.72 (m, 1H), 2.48 (m, 1H). ^{13}C NMR ($CDCl_3$). δ (ppm) = 177.7, 131.9, 131.1, 129.6, 128.5, 118.4, 107.2, 49.2, 41.1, 39.7. HR-MS Calcd for $C_{10}H_{10}INO$: 286.9807. Found: 286.9821.

3.5. Preparation of 4-(5-(dimethylamino)naphthalene-1-sulfonamido)-3-(4-iodophenyl)-butanoic acid (*4*)

A solution of lactam **10** (86 mg, 0.3 mmol) in 5 N HCl (3 mL) was heated at 100 °C for 18 h. The excess of water in the reaction mixture was removed under reduced pressure. A mixture of dansyl choride (81 mg, 0.3 mmol) in acetonitrile (2 mL) was added, followed by potasium carbonate (170 mg) in water (4 mL). The reaction mixture was stirred at room temperature for 6 h and extracted with dichloromethane. The combine organic solution was washed with HCl (pH 2, 5 mL). After evaporation of the solvent, the crude was purified by silica gel flash column chromatography to give a yellow solid (160 mg, 89%). ^{1}H NMR ($CDCl_3$). δ (ppm) = 8.24 (m, 2H), 8.00 (m, 1H), 7.57 (m, 3H), 7.15 (m, 1H), 6.92 (m, 2H), 6.62 (m, 1H), 3.59 (m, 1H), 3.35 (m, 1H), 3.41 (m, 1H), 2.85 (s, 6H), 2.62 (m, 1H), 2.48 (m, 1H). HR-MS Calcd for $C_{22}H_{23}IN_2O_4S$: 538.0423. Found: 538.0435.

Human breast cancer cell line MCF-7 was grown in RPMI 1640 medium with 10% fetal calf serum at 37 °C in 5% CO_2. For induction of apoptosis, the cells were treated with 40 nM paclitaxel for 16 h. Then treated cells were washed with PBS twice prior to being incubated with DNSBA (50 μM) and Annexin V-Alexa®488 for 20 min at RT. The cells stained with Alexa®488-labeled Annexin V and DNSBA were observed using an Applied Spectral Imaging (ASI, Migdal Ha'Emek, Israel) platform. The corresponding filters with excitation at 300–400 nm and emission at 445–480 nm were employed for the detection of DNSBA, whereas the filters with excitation at 480–505 nm and emission at 510–550 nm were used for Alexa®488

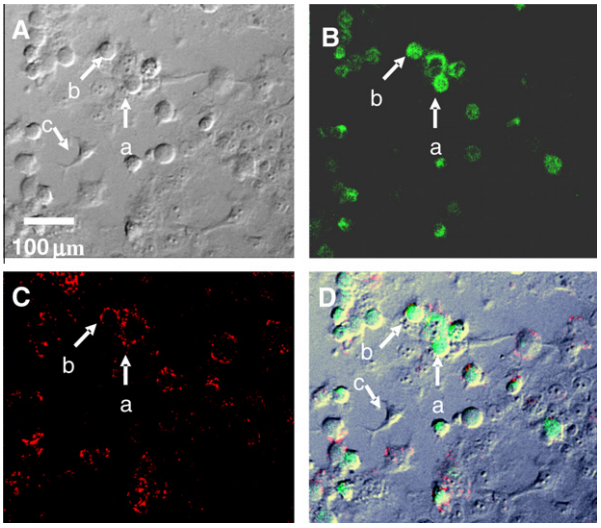

Fig. 1. Images in the same field of view of treated MCF-7 cells dually stained with Alexa®488 labeled Annexin V and DNSBA (**1**). (A) DIC image; (B) DNSBA in green; (C) Alexa®488 in red; (D) composite image of (A), (B), and (C). 100× total magnification. (For interpretation of the references to color in this figure legend, the reader is referred to the web version of this article.)

detection. In addition, a third image in the same field of view was acquired by differential interference contrast (DIC) to reveal cell structure and morphology. Each image was then presented individually and an overlay of the fluorescent images with DIC was created to demonstrate the location of both fluorophores into the cells.

The biological evaluation demonstrated that healthy MCF-7 cells were not stained with either DNSBA or Annexin V. When the cells were treated with 40 nM paclitaxel for 16 h, about 40–50% of the cells undertook a round morphology, which was indicative of the induction of apoptosis [Fig. 1A, a and b identify apoptotic cells, and c identify actively growing (spreading and dendritic) cell]. These abnormal round cells were stained by DNSBA (Fig. 1B) and Annexin V (Fig. 1C). The detection signals of DNSBA and Annexin V were largely overlapped on the periphery of the rounded MCF-7 cells (Fig. 1D).

High magnification imaging (Fig. 2, resolution: 20 μm) clearly showed that Annexin V binds to the surface, while DNSBA accumulated inside the cytoplasm of the apoptotic cells.

These imaging clearly confirmed that DNSBA could be used as a probe for *in vitro* imaging of apoptosis. However, use of Annexin as an imaging strategy requires a separate, *in vitro* test, using propidium iodide (PI) to distinguish between apoptosis (membrane intact) and necrosis (membrane damaged) [22–24]. Importantly, Annexin V detects the early stage of apoptosis since its binding of PS externalization period is a relatively early event in apoptosis. For further investigation to detect the different stage of apoptosis with DNSBA, the parallel experiments with SYTOX® Orange staining were carried out. SYTOX® Orange can be used to define late-stage apoptotic cells, since it binds to the nucleus of the late-stage dead cells with broken membranes. Co-staining of DNSBA with SYTOX® Orange showed that DNSBA binds to either the early or the late-stage apoptotic cells [Fig. 3, a identify a spreading actively growing cell, b identify a late-stage apoptotic cell in which the nucleus can be stained with SYTOX® Orange (in red[1]); and c identify an early or middle stage apoptotic cell in which the nucleus is not stained by SYTOX® Orange]. Therefore, DNSBA could be used to detect all stages of apoptotic cells, confirmed by the Annexin Alexa®488 staining and SYTOX® Orange staining. The development of a non-invasive *in vivo* imaging protocol that can detect the apoptotic process in different diseases, and can be used to monitor the ability of a drug to either induce or inhibit apoptosis, would be of enormous value to the medical community [3,25]. Additional experiments showed that DNSBA detects the chemotherapy-induced apoptotic cells of other human cancer cell lines including HT-29 colon carcinoma and K562 leukemia (unpublished data).

[1] For interpretation of color in Figs. 1–3, the reader is referred to the web version of this article.

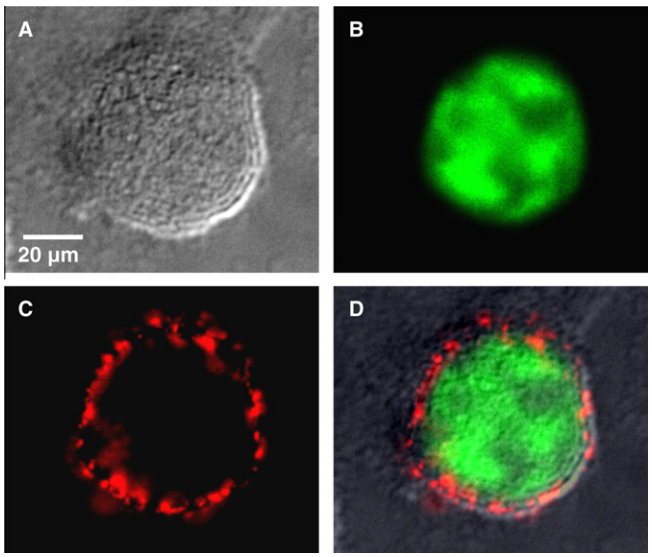

Fig. 2. High resolution images in the same field of view of treated MCF-7 cell dually stained with Alexa®488 labeled Annexin V and DNSBA (**1**). (A) DIC image; (B) DNSBA in green; (C) Alexa®488 in red; (D) composite image of (A), (B), and (C). 600× total magnification. (For interpretation of the references to color in this figure legend, the reader is referred to the web version of this article.)

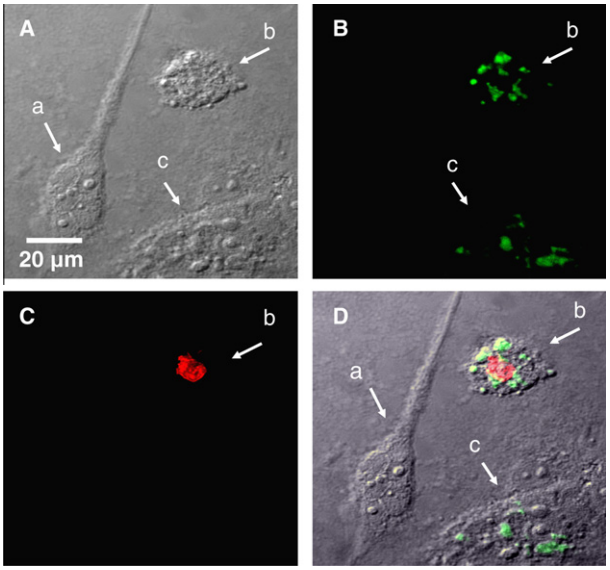

Fig. 3. Images in the same field of view of treated MCF-7 cells dually stained with DNSBA and SYTOX® Orange. (A) DIC image; (B) DNSBA in green; (C) SYTOX® Orange in red; (D) composite image of (A), (B), and (C). 600× total magnification a identify a spreading actively growing cell, b identify a late stage apoptotic cell in which the nucleus can be stained with SYTOX® Orange (in red); and c identify an early or middle stage apoptotic cell in which the nucleus is not stained by SYTOX® Orange. (For interpretation of the references to color in this figure legend, the reader is referred to the web version of this article.)

4. Discussion

Ziv et al. reported that dansyl compounds NST-732 (**2**) can be used for imaging apoptosis process in three experimental, clinically

relevant animal models of: renal ischemia/reperfusion, cerebral stroke, and irradiation treated lymphoma [10,15,25,26]. The NST-732 (**2**) showed high sensitivity and specificity in targeting apoptotic cells *in vivo* in all three models used. Uptake of NST-732 (**2**) in apoptotic cells was higher than in the non-apoptotic ones, and the specificity of NST-732 (**2**) targeting was demonstrated by its localization in regions of apoptotic/necrotic cell death, detected morphologically and by TUNEL staining. To date, only fluorine-18 labeled dansyl derivatives have been reported. In this work, DNSBA was designed to facilitate radioiodine labeling which could be used for both SPECT and PET imaging. Our results clearly show that **4** detects apoptotic cancer cells induced by treatment with chemotherapeutic drugs such as paclitaxel. In these experiments, we found that **4** does not distinguish early stage apoptosis from late-stage apoptosis and could be used to detect all stage of apoptotic cells. Moreover, this does not affect their potential use of the reagent in evaluation treatment efficacy since both early and late apoptotic cells are indicative of positive signals of effective treatment. Because of its inherent fluorescence feature, the DNSBA can be convenient used for *in vivo* optical apoptosis imaging.

5. Conclusion

In summary, we have accomplished the synthesis of a dansyled amino acid, DNSBA, in good yield. The biological evaluations of DNSBA show that it selectively binds to paclitaxel-induced apoptotic cancer cells, and exhibits intracellular uptake and accumulation in apoptotic cells. Though DNSBA could not differentiate the early stage and final stage of apoptosis from necrosis, it shows the ability to detect multiple pathways leading to cell death may be advantageous in the evaluation of cancer treatment indicative of a positive therapeutic outcome. The probe allows users to identify apoptotic cells with a broaden scope of the detection when compared with gold standard-Annexin V. These small-molecule-based apoptosis detecting probes are of great value for cancer treatment evaluation as well as other medical applications.

Acknowledgments

This research was supported by the Program of New Century Excellent Talents in University (NCET-09-0800), National Natural Science Foundation of China (No. 30900377), and the Physician's Medical Education and Research (PMERF).

References

[1] H. Steller, Mechanisms and genes of cellular suicide, Science 267 (1995) 1445–1449.
[2] F. Blankenberg, P. Katsikis, J. Tait, R. Davis, L. Naumovski, K. Ohtsuki, S. Kopiwoda, M. Abrams, H. Strauss, Imaging of apoptosis (programmed cell death) with 99mTc Annexin V, J. Nucl. Med. 40 (1999) 184–194.
[3] J. Hakumaki, T. Liimatainen, Molecular imaging of apoptosis in cancer, Eur. J. Radiol. 56 (2005) 143–153.
[4] J. Tait, Imaging of apoptosis, J. Nucl. Med. 49 (2008) 1573–1576.
[5] M. Corsten, L. Hofstra, J. Narula, C. Reutelingsperger, Counting heads in the war against cancer: defining the role of Annexin A5 imaging in cancer treatment and surveillance, Cancer Res. 66 (2006) 1255–1260.
[6] Q. Luo, Z. Zhang, F. Wang, H. Lu, Y. Guo, R. Zhu, Preparation, *in vitro* and *in vivo* evaluation of (99m)Tc–Annexin B1: a novel radioligand for apoptosis imaging, Biochem. Biophys. Res. Commun. 335 (2005) 1102–1106.
[7] W. Shynkar, A. Klymchenko, C. Kunzelmann, G. Duportail, C. Muller, A. Demchenko, J. Freyssinet, Y. Mely, Fluorescent biomembrane probe for ratiometric detection, J. Am. Chem. Soc. 129 (2007) 2187–2193.
[8] P. Meers, T. Mealy, Calcium-dependent Annexin V binding to phospholipids: stoichiometry, specificity, and the role of negative charge, Biochemistry 32 (1993) 11711–11721.
[9] H. Boersma, B. Kietselaer, L. Stolk, A. Bennaghmouch, L. Hofstra, J. Narula, G. Heidendal, C. Reutelingsperger, Past, present, and future of annexin A5: from protein discovery to clinical applications, J. Nucl. Med. 46 (2005) 2035–2050.
[10] D. Zhou, W. Chu, J. Rothfuss, C. Zeng, J. Xu, L. Jones, M. Welch, R. Mach, Synthesis, radiolabeling, and *in vivo* evaluation of an ^{18}F-labeled isatin analog for imaging caspase-3 activation in apaptosis, Bioorg. Med. Chem. Lett. 16 (2006) 5041–5048.
[11] R. Aloya, A. Shirvan, H. Grimberg, A. Reshef, G. Levin, D. Kidron, A. Cohen, I. Ziv, Molecular imaging of cell death *in vivo* by a novel small molecule probe, Apoptosis 11 (2006) 2089–2101.
[12] W. Wang, S. Kim, W. El-Deiry, Small-molecule modulators of p53 family signaling and antitumor effects in p53-deficient human colon tumor xenografts, Proc. Natl. Acad. Sci. U.S.A. 103 (2006) 11003–11008.
[13] K. Kim, M. Lee, H. Park, J. Kim, S. Kim, H. Chung, K. Choi, I. Kim, B. Seong, I. Kwon, Cell-permeable and biocompatible polymeric nanoparticles for apoptosis imaging, J. Am. Chem. Soc. 128 (2006) 3490–3491.
[14] K. Bullok, D. Piwnica-Worms, Synthesis and characterization of a small, membrane-permeant, caspase-activatable far-red fluorescent peptide for imaging apoptosis, J. Med. Chem. 48 (2005) 5404–5407.
[15] M. Swairjo, B. Seaton, Annexin structure and membrane interactions: a molecular perspective, Annu. Rev. Biophys. Struct. 23 (1994) 193–213.
[16] A. Reshef, A. Shirvan, H. Grimberg, G. Levin, A. Cohen, A. Mayk, D. Kidron, R. Djadetti, E. Melamed, I. Ziv, Novel molecular imaging of cell death in experimental cerebral stroke, Brain Res. 1144 (2007) 156–164.
[17] W. Zeng, M. Yao, D. Townsend, G. Kabalka, J. Wall, M. Le Puil, J. Biggerstaff, W. Miao, Synthesis, biological evaluation and radiochemical labeling of a dansylhydrazone derivative as a potential imaging agent for apoptosis, Bioorg. Med. Chem. Lett. 18 (2008) 3573–3577.
[18] W. Zeng, D. Townsend, G. Wall, W. Miao, Biological evaluation of dansylhydrazone derivatives for cancer cell apoptosis imaging, J. Nucl. Med. 49 (2008) S351.
[19] W. Zeng, W. Miao, G. Kabalka, M. Le Puil, M. Biggerstaff, D. Townsend, Design, synthesis, and biological evaluation of a dansyled amino acid derivative as an imaging agent for apoptosis, Tetrahedron Lett. 49 (2008) 6429–6433.
[20] E. Corey, F. Zhang, Enantioselective Michael addition of nitromethane to alpha, beta-enones catalyzed by chiral quaternary ammonium salts. A simple synthesis of (*R*)-baclofen, Org. Lett. 2 (2000) 4257–4259.
[21] G. Kabalka, G. Tang, A. Mereddy, No-carrier-added radiohalogenations utilizing organoborates, J. Labelled Compd. Rad. 50 (2007) 446–447.
[22] G. Tang, W. Zeng, M. Yu, G. Kabalka, Facile synthesis of *N*-succinimidyl 4-[18F]fluorobenzoate ([18F]SFB) for protein labeling, J. Labelled Compd. Rad. 51 (2008) 68–71.
[23] G. Smith, Q.D. Nguyen, E.O. Aboagye, Translational imaging of apoptosis, Anti-Cancer Agents Med. Chem. 9 (2009) 958–967.
[24] W. Zeng, W. Miao, Development of small molecular probes for the molecular imaging of apoptosis, Anti-Cancer Agents Med. Chem. 9 (2009) 986–995.
[25] H. Grimberg, G. Levin, A. Shirvan, A. Cohen, M. Yogev-Falach, A. Reshef, I. Ziv, Monitoring of tumor response to chemotherapy *in vivo* by a novel small-molecule detector of apoptosis, Apoptosis 14 (2009) 257–267.
[26] M. Damianovich, I. Ziv, S. Heyman, S. Rosen, A. Shina, D. Kidron, T. Aloya, H. Grimberg, G. Levin, A. Reshef, A. Bentolila, A. Cohen, A. Shirvan, Aposense: a novel technology for functional molecular imaging of cell death in models of acute renal tubular necrosis, Eur. J. Nucl. Med. Mol. Imaging 33 (2006) 281–291.